INTERNATIONAL ATOMIC ENERGY AGENCY
UNITED NATIONS EDUCATIONAL, SCIENTIFIC AND CULTURAL ORGANIZATION
INTERNATIONAL CENTRE FOR THEORETICAL PHYSICS
I.C.T.P., P.O. BOX 586, 34100 TRIESTE, ITALY, CABLE: CENTRATOM TRIESTE

UNITED NATIONS INDUSTRIAL DEVELOPMENT ORGANIZATION

INTERNATIONAL CENTRE FOR SCIENCE AND HIGH TECHNOLOGY

H4.SMR/540-16

Second Training College on Physics and Technology of Lasers and Optical Fibres

21 January - 15 February 1991

Lasers in Medicine

R. Salimbeni
Istituto di Elettronica Quantistica del CNR
50127 Firenze, Italy

Lasers in Medicine

Renzo Salimbeni

Istituto di Elettronica Quantistica del CNR
Via Panciatichi 56/30
50127 Florence, ITALY

Contents.

Introduction.

The aim of this lecture is to provide a brief description of the basic concepts laying behind both the experimental and the everyday utilizations of lasers in biomedical fields. To this purpose it is worth to recall the radiation characteristics and the technology of the lasers so far employed in surgery. Then a chapter devoted to the presentation of the classes of independent photophysical processes which can be excited by the laser radiation is following. A description of the delivery systems introduces to the presently ongoing biomedical application fields, underlining here that only basic concepts and physical issues will be considered, relying, for the clinical side, on specific medical reports.

1. Laser radiation characteristics

1.1 Main parameters of the emission

Besides the well known popularity of the LASER in the people imagination, not all its radiation properties are known as well. First of all it is worth to be noted that laser action can be obtained in almost every material within the proper operating conditions. The "active medium" can be in solid, liquid or gaseous phase. The transition can be rotational, vibrational, or electronic, atomic or molecular, to the extent that nowadays thousands of different laser wavelength are available. All of them share the more or the less some very attracting basic characteristics:

1) monochromaticity, due to the high selection imposed by the oscillating cavity, a few Mhz is the frequency broadening of a typical single mode laser operation,

2) spatial and temporal coherence, due to the large grade of correlation between the stimulated emissions at different sites of the medium, providing for example well defined interference between overimposed beams (holography),

3) directionality, generally depending on the resonator properties, it is possible to emit beams at the diffraction limit related to the finiteness of the size, that is better evaluated considering a gaussian beam of 10 cm @ 500 nm, in this example the beam can propagate with a limited divergence of only 6 mm every Km.

Very important is to consider also the type of emission, which can be continuous or pulsed. In this case the duration of the emission can vary according to the excitation duration (from mS to nS), to a sudden clearance of the oscillating cavity for Q-switch operation or cavity damping (from μS to nS), or inducing a phase modes locking to get roughly the inverse of the Fourier transform of the oscillating bandwidth (down to pS for wideband amplifying media such as Dyes).

For CW lasers the power of the radiation defines completely the energy content. For pulsed lasers a peak power can be defined, a pulse duration is usually given at half maximum (FWHM), a repetition rate of the pulses determines an average power as the product of the

single pulse energy times the rep rate. The energy and the power densities are usually important. Determined by the typically small focal spot in which the beam is concentrated by a proper lens, they can reach up to hundreds of J/cm^2 and MW/cm^2 respectively.

2. The technology of surgical lasers.

Out of the number of different laser types we would consider in this chapter the more relevant ones for surgical purpose, meaning in other words the lasers which have been proposed and employed to perform typical surgical aims: tissue cut, tissue removal, photocoagulation, and others.

2.1 The CO_2 laser

This class of lasers was discovered by Patel in 1964. The active medium consists of molecules of carbon dioxide excited directly or through an almost resonant energy transfer mechanism with nitrogen molecules. The transition takes place between different vibrational states of the molecule, from an asymmetric stretching mode to a symmetric stretching. This level system determines an emission wavelength in the infrared near 10 μm. This laser is inherently characterized by a quite high quantum efficiency which is reflected, in practical devices, in a considerably high overall efficiency, typically of the order of 20-30%. No bottle neck occurs in the arrival state of the transition due to collision-excitation with other molecules, so that cw emission is possible and it is in fact obtained in relatively simple devices. The technology of the systems consists in a glass tube, usually with double wall to obtain outer cooling water circulation, in which a gas mixture (CO_2, N_2 He = 4.5%: 13.5%: 82%) is slowly flowing at a pressure of 20-30 torr with the aid of a vacuum pump. The excitation discharge takes place longitudinally between electrodes set at the extremes of the tube (usually 5-10 kv and 0.3-0.5 A) providing collisional electronic excitation for the CO_2 molecules. The mirrors in the most simplified versions are integral part of the tubes providing as well tight vacuum sealing. The operating parameters are not critical at all, and indeed CO_2 lasers are pretty simple to keep working. The emission can be a typical TEM_{00} with output power in the order of 50-100 W from a less then a meter long device. Pulsed excitation versions provide eventual pulses with an increased power to 200-300 W for a fraction of a ms. The power level can be easily adjusted in a current control mode. These notes are typically describing the size and the performance of CO_2 lasers for biomedical applications but it is worth to be noted that the CO_2 laser lends itself to large scale devices even up to 10 KW output power for industrial purposes. Fig. 1 shows a typical system. A suitable beam delivery system can be observed and this will be described in some detail later. The beam arrives at an handpiece through a final lens to determine a focal spot of ~1 mm at a few mm out of the piece. In this spot a power density in the order of 5 KW/cm^2 is reached, which is enough to vaporize every organic substance.

2.2 The Ar ion laser

Ion lasers are the most powerful CW laser sources in the visible. The Argon ion laser is

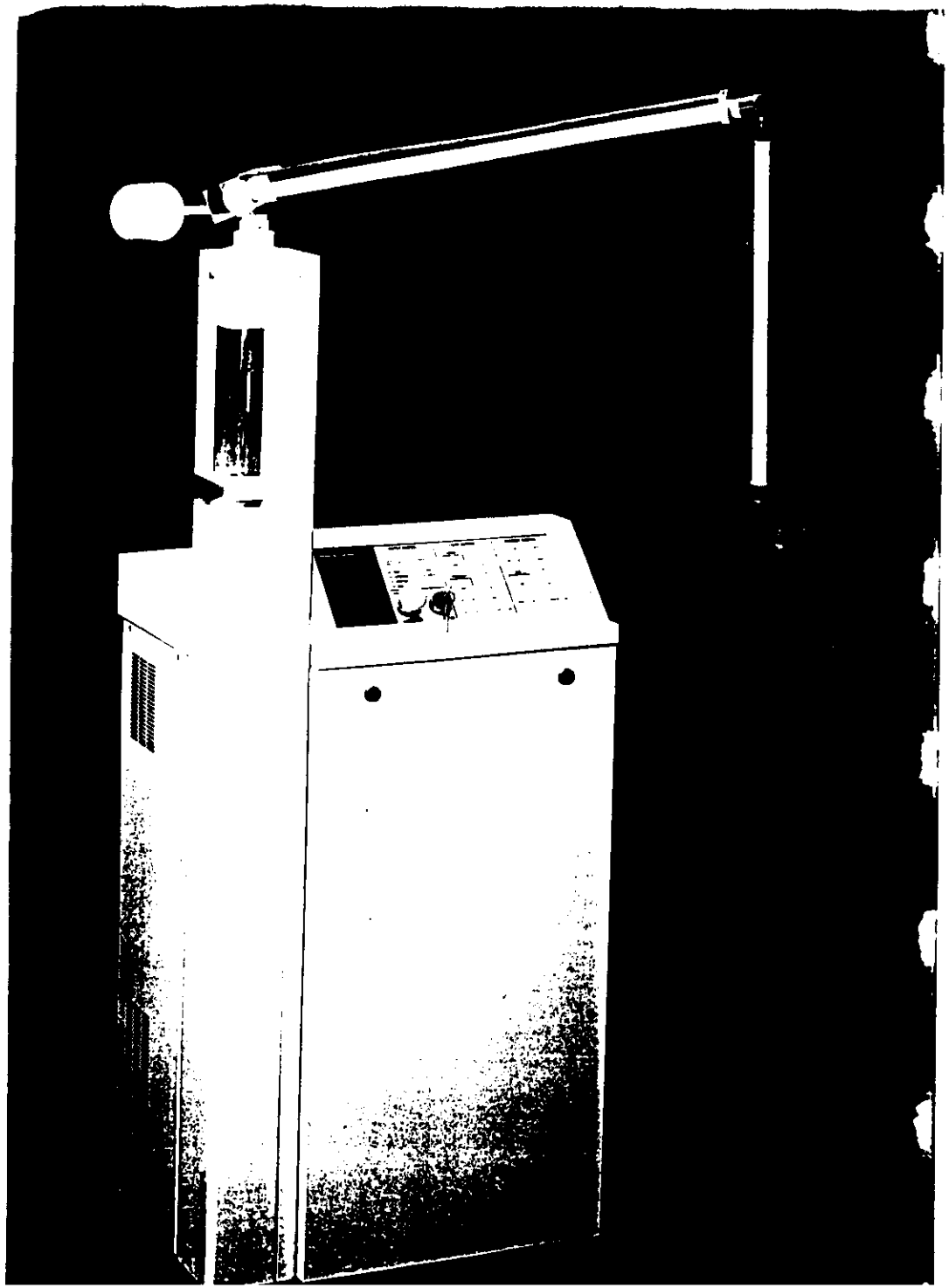

the best known of this class. Fig. 2 shows the energy levels diagram. As it can be noted the laser transition takes place between very high energy levels (35 eV). So that a large energy is required to create an upper level population. A two steps excitation is usually provided to first ionize and then to rise to the upper levels of the ion. A strong vacuum UV transition drains the lower laser level population and a population inversion occurs. In symbols if N is the population of ions in the upper level

$n_e = n_i$ charge neutrality condition

$N \propto n_e^2 \propto i^2$ so a quadratic current dependence of the upper laser level population comes out.

The engineering in these devices had to provide first these high current densities, solving all the problems regarding the material selection for the consequent high temperature operation. Usually a special material tube (BeO_2) or a set of graphite discs, delimit the dimension of the discharge current flow. A suitable longitudinal magnetic field, reducing the electrons and ion collisions to the wall of the capillary tube and increasing both current density and laser power without increasing the operating temperature. The laser emission divides the CW power of several W to a maximum of ~20 W in 2 fundamental lines at 4880 Å and 5145 Å and a set of other lines. A reliable TEM_{00} operation is typical for these devices which, as a matter of facts, have been an invaluable tool for so many applications, from holography to industrial ones, from biomedical to space, LIDAR and more.

2.3 The Nd:YAG and other S.S.L.

An intrinsic advantage of the location of suitable ions in a crystalline host structure is represented by the very high concentration which can be reached $10^{26}/m^3$ compared to $10^{23}/m^3$ of gases. Several ions and different hosts provide a set of different combinations: Neodymium, Herbium, Holmium, Thulium, and Chromium can be hosted in Yttrium Scandium Gadolinium Garnets (YSGG). Other SSL have a very wideband homogeneously broadened gain allowing an efficient tuning of the oscillating frequency. They are called vibronic lasers. The best known are the Alexandrite SSL (Cr^{3+}:$BeAl_2O_4$), the Titanium Sapphire (Ti:Al_2O_3). Tab.1 represents the wavelength emitted from all these solid state lasers. Fig.3 presents a typical configuration of a flashlamp pumped SSL. These lasers can operate in the usual "free running modes" operation, or in especially tailored short pulsewidth operations. In fact Nd:YAG and many other can be excited by flashlamps in both CW and pulsed emission. In the free running modes the pulsewidth is typically a few μseconds. In a pulsed operation a Q-switched option for the resonator induces the emission to be restricted in a much shorter duration (10-100 ns depending on the laser medium) and an extremely high peak power. An eventual mode locking in the optical cavity can induce the emission to come out as a train of ultrashort pulses (10-100 ps).

2.4 The metal vapor laser

This class of lasers uses metal atoms in their first electronic states as the active medium. Fig.4 shows the typical energy level diagram for copper. An immediate observation regards the relatively low energy needed to create an excited state. Due to the high quantum efficiency

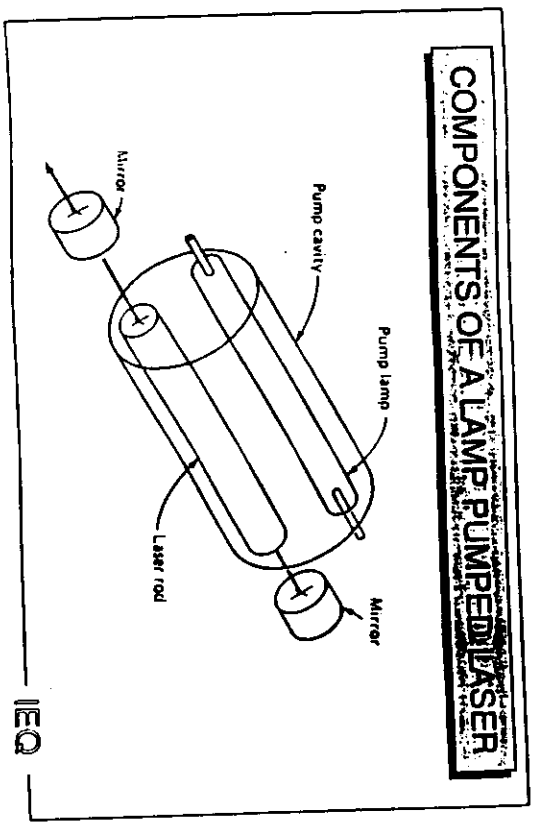

Fig. 3

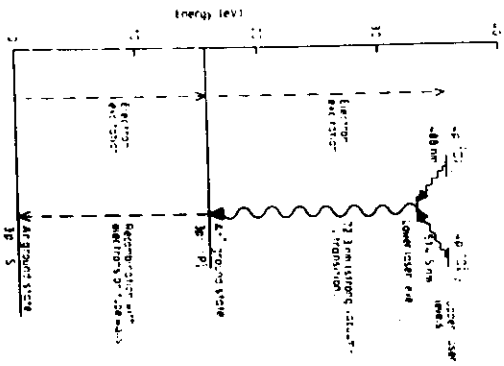

Figure 2 Energy level diagram of the principal argon-ion laser transitions.

Table 1
Various solid-state laser systems

Host	Dopant	Sensitizer	Popular name	Laser wavelength [μm]	Performance	Efficiency [%]	Operating temperature [K]	Pump source	Reference
$YAlO_3$	Nd^{3+}	Cr	YALO YAP	1.064	225 mJ/pulse, Q-switched 20 ns 10 pps	0.4	300	Xenon flashlamp	[2.105]
					110W cw	1	300	cw krypton	[2.106]
$CaLa_4(SiO_4)_3O$	Nd^{3+}	—	SOAP	1.061	500 mJ/pulse, Q-switched 30 ns 30 pps 6 mm × 75 mm rod	1	300	Xenon flashlamp	[2.21, 2.23]
$Y_3Al_5O_{12}$	Ho^{3+}	Er–Tm	YAG	2.1	rod size 3 × 50 mm 20 W cw	4	77	Tungsten–iodine	[2.13]
$YLiF_4$	Ho^{3+}	Er–Tm	YLF	2.06	4 mJ Q-switched 150 mJ long pulse (2 μs) 3 mm × 20 mm rod	0.5	300	Xenon flashlamp	[2.35]
$YLiF_4$	Er^{3+}	—	YLF	0.85	60 mJ/pulse, long pulse 5 mm × 30 mm rod, threshold (10–100) J	0.03	300	Xenon flashlamp	[2.35]
$YAlO_3$	Er^{3+}	—	YALO	1.66	6 mm × 50 mm rod, threshold 52 J	—	300	Xenon flashlamp	[2.18]
Glass	Er^{3+}	Yb	Glass	1.54	4 mm × 76 mm rod	0.25	300	Xenon flashlamp	[2.7]
					output 0.85 J (conventional) 0.18 J (Q-switched)	0.1	300		
$YAlO_3$	Tm^{3+}	Cr	YALO YAP	2.35	5 mm × 50 mm rod Threshold at 110 J	—	300	Xenon flashlamp	[2.48]
$YLiF_4$	Nd^{3+}	—	YLF	1.053	5 mm × 50 mm rod, threshold 8 J slope eff. 0.8%, output 200 mJ pulse width 100 μs	0.7	300	Xenon flashlamp	[2.36]
$La_2Be_2O_5$	Nd^{3+}	—	BEL	1.070	5 mm × 50 mm rod output 9 W cw	0.33	300	Tungsten–iodine	[2.33]

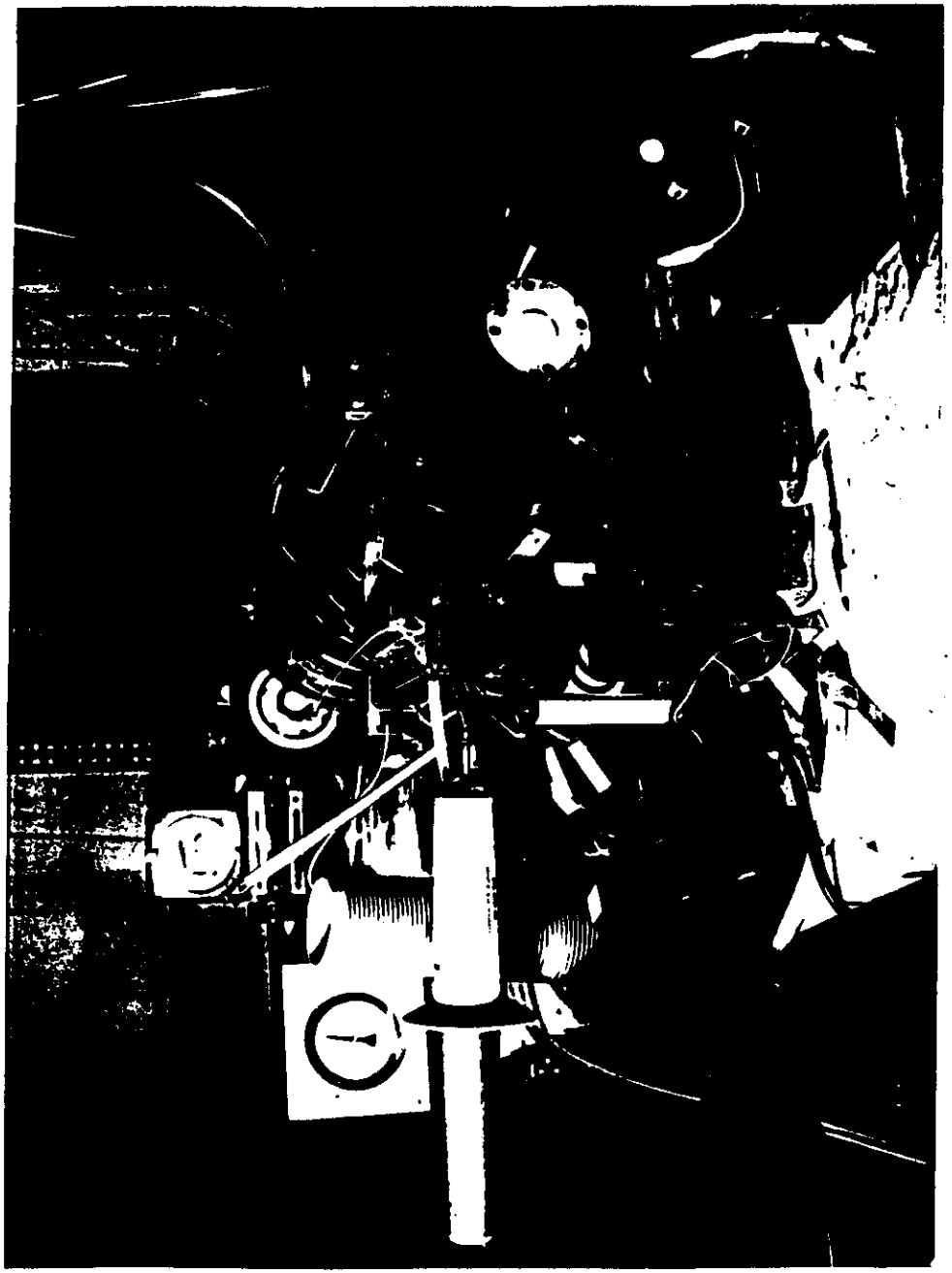

Fig. 5

this atomic transition takes place with an intrinsically high efficiency decaying on a metastable level. This characteristic determines a "bottle-neck" effect to the transition which remains self-terminated whenever the papulation in this arrival state destroys the population inversion. The operating regime is necessarily pulsed. The transition is split in two main lines at 510 and 518 nm. The active medium is arranged in a vapor column typically 2-4 cm in diameter times 50-150 cm in length, contained within a ceramic alumina cylinder, in which a suitable heater keeps a constant temperature around 1500°C to achieve copper vapor pressure of a fraction of a mbar. A typical system is shown in Fig.5. The excitation circuit provides a current pulse of a few KA lasting for tens of ns. The high excitation rate and the large atoms density determines a very high gain and a pulsed operation with a small energy per pulse ~1-10 mJ and a duration of 10-50 ns. In practical devices the excitation discharge is repeated 5-10 thousands times/second providing an input average power in the order of some KW to the active volume. If this is thermally insulated the temperature can rise up to the desired level of 1500°C (to 1600°C for gold vapor operation). In this way the device can operate with a reasonably high efficiency emitting average power ranging from 10-100 W on both the green and the yellow lines. Gold vapor versions are less efficient but still emit more than 10 W @ 630 nm. This low cost visible radiation (comparing with the Argon ion laser for example) is used directly or it lends itself for pumping dye lasers. This lasers combination produces several watts of tunable laser power amenable for many applications: photochemistry, photobiology, photodynamic therapy and more.

2.5 The Dye lasers

This class of lasers represents the first successful system providing to the experimenters the right wavelength for every purpose! This is in facts a tunable laser system employing as an active medium organic molecules which are dyes usually involved in industrial coloring. These molecules present in their structure a relevant number of conjugated bonds determining an homogeneous vibrational and rotational broadening of the electronic states. This typical levels situation is reported in Fig.6. The excitation can be provided by flashlamps or lasers to a proper solution of these organic dyes (Rhodamines, Coumarines, and other) in suitable solvents (ethyl alcohol, water) flowing in glass or quartz cells. CW operation is possible pumping with an Argon laser in focal spot irradiating a dye jet to provide the power density of 10^8 W/m^2 necessary to overcome the oscillation threshold. Several versions use nitrogen or excimer laser radiation, and frequency doubled Nd:YAG radiation in a transverse geometry to pump oscillator + amplifier configurations. They share the common characteristic to host in the resonator a dispersive element (a prism, a grating or interferometers) to select the desired wavelength with the minimum resonator losses. Fig.7 presents the tuning curves of the main dyes.

2.6 The Excimer lasers

These lasers have been discovered in the middle 70's in studies searching for high efficiency UV lasers. Indeed these very short living excited dimers (exci-mers) can be efficiently formed by the collision of excited or ionized rare gas atoms with an halogen bearing molecule. The strong ionic field causes an harpooning mechanism which easily create a rare

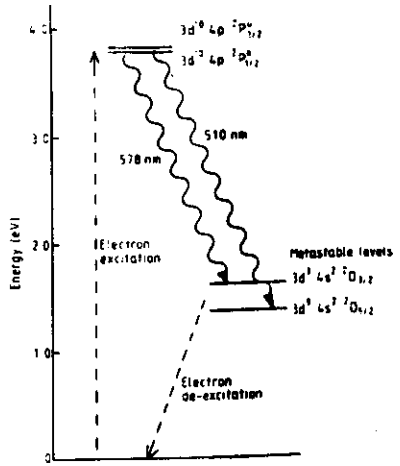

Figure 4 Energy level diagram of copper-vapour laser transitions.

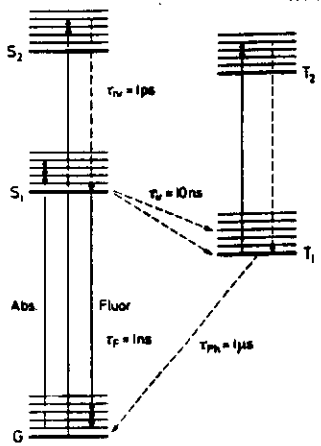

Fig. 6 Eigenstates of a typical dye molecule with radiative (solid lines) and non-radiative (broken lines) transitions

FIG. 7

Dye Conversion Efficiency Curves
Shown below are provisional performance curves when the EXC-1 is used to pump the PDL-1E dye laser. Contact Quanta-Ray for more specific information.

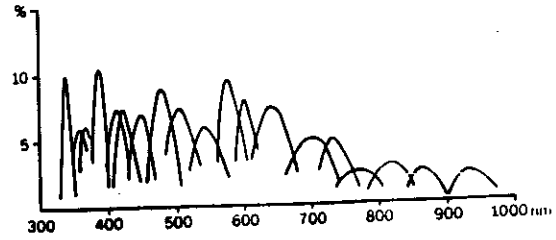

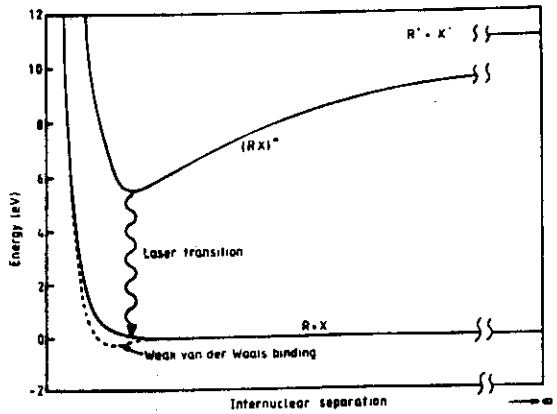

Figure 8 Potential-energy diagram of a typical rare-gas halide.

Tabella 2.

Lunghezza d'onda di emissione laser (L) o di fluorescenza (F) di alcuni eccimeri (λ in nm)				
Eccimeri di gas rari λ Xe_2 172(L) Kr_2 146(L) Ar_2 126(L)				
	Alogenuri di gas rari			
	F	Cl	Br	I
Ar	193(L)	175(L)	PRED	N.I
Kr	249(L)	223(L)	203(F)	PRED
Xe	352(L)	308(L)	282(L)	253(F)

L osservata emissione laser
F osservata solo fluorescenza
PRED stato eccitato predissociativo
N.I livello inferiore dello stato eccitato non ionico

gas halide. Typical examples are all the combinations between Ar, Kr, and Xe with Br, Cl, and F. The laser transition arrives on a dissociating ground state which releases the two atoms. The level scheme is reported in Fig.8. The pumping kinetic is greatly improved by a third constituent a buffer gas, so that a typical mixture of Xe, Hcl, and Ne (0.1:1:98.9) is employed to obtain the XeCl excimer. This mixture is excited by a high voltage (10-30 KV) and high current (several KA) discharge or by e-beam. The former type gives more compact and reliable devices. They typically emit pulses of 100 mJ-1J energy and 10-100 ns duration. Table 2 shows the emission wavelengths for the different rare gas halides. After 15 years of development the technology of these devices is still improving, considering that only recently several industrial and medical applications have shed light on the limitations of present devices.

2.7 The Semiconductor lasers

A very promising class of solid-state lasers for biomedical applications is represented by the new generation of semiconductor lasers. Fig.9 provides a general scheme to explain the typical situation. Here a population of electrons is located in a P-region with a greater energy than the electrons in the N-region. If an electric field is applied on the p-n junction the electrons flow from n to the p and similarly the holes. They eventually recombine releasing an optical radiation with eV > 4 > Eg. The wavelength is typically ranging between 0.8 and 1.3 μm for double heterojunction such as AlGaAs or InGaAsP. Other IV-VI compounds (PbCdS, Pb, GeS and other) can provide emission from 2.5 to 33 μm. For shorter wavelengths GaInAsP has the potential to emit red radiation around 650 nm.

Power levels are improving using laser diode arrays. Tens of watts are commercially available and surface emitting diodes are expected to reach KW operation. Considering the great efficiency (> 20%) laser diode arrays are amenable for side pumping of Nd:YAG crystals in close coupled arrangements which turn out in very compact, high beam quality, high efficiency "miniature lasers". An intracavity frequency doubler can convert in the green the emission increasing considerably the range of application. In conclusion diode lasers are rapidly becoming an attractive alternative to other solid state or gas lasers.

3. Photophysical processes in laser-tissue interaction

3.1 Introduction

Extensive reviews of the principal photobiologic interactions between nonionizing radiation and living tissues have been made both for the submillimeter part of electromagnetic spectrum and the optical region. In the specific case of laser radiation, the unique characteristic of monochromaticity of the incident field and the spatial and temporal coherence of the emission, find increasing use in medical applications, in both diagnosis and therapy. Together with the resulting biologic response of the irradiated tissues, these characteristics determine the specific modes of interaction, namely, the various processes of conversion of the incident electromagnetic energy within biomolecules. Fig.10 shows a plot of power density and interaction time for different effects.

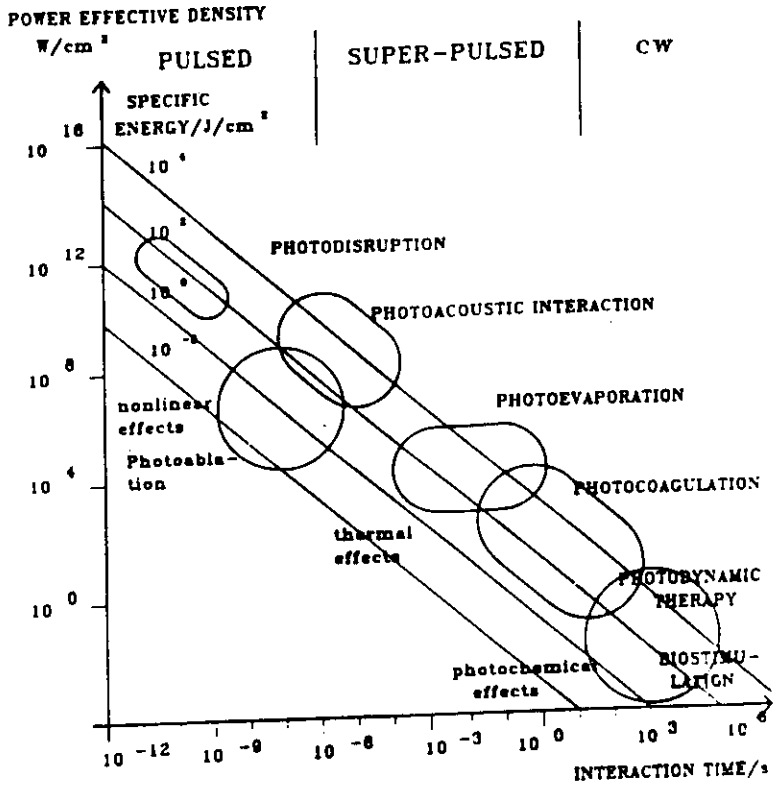

Fig. 10 Different laser tissue interactions as a function of interaction time and power density. The specific energy is the field parameter.

Considering the large range of time scales associated with the foregoing photomedical applications (more than 12 decades), the relatively small dispersion of the energy fluence (3-4 decades) corresponding to specific photoresponses seems to substantiate the proposal that irradiance and light exposure periods can be varied compensatively. In effects every irradiance level determines a sum of effects in which one is the main and others are present anyway.

3.2 Photothermal

All laser surgical applications, whether in the cutting or hemostatic mode, rely upon the conversion of electromagnetic energy to thermal energy. This is achieved by focusing a beam onto spot sizes of few micrometers or millimeters wide; such collimation is possible because of the spatial coherence of lasers which can supply high energy densities providing spatially confined heating of target tissues, resulting in thermal injury, tissue removal, or control of bleeding. The choice of wavelength determines the depth of penetration and thus influences the interplay between tissue removal and hemostasis.

In fact, the vast majority of therapeutic applications of lasers takes advantage of their capability for some spatial control over the degree and extent of tissue injury. The characterization of the photothermal biologic response following laser irradiation depends, however, on the structural level that is targeted.

At the microscopic level, the photothermal process originates from the bulk absorption occurring in molecular vibration-rotation bands or, perhaps, in the vibrational manifold of the lowest electronic excited state, instantaneously followed by subsequent rapid thermalization through nonradiative decay. Since tissue structures may be considered as a complex condensed phase media, rotation is hindered and vibration amplitudes are more or less damped; consequently, energy levels are not sharp but instead are broadened. It is then more appropriate to describe vibrationally excited electronic states in terms of vibronic states. The reaction with a target molecule A proceeds in two nearly simultaneous steps: first, the absorption of a photon of energy hν, promoting A to a vibronic state A^*; second, an inelastic scattering occurring on a 1-100 psec time-scale with a collisional partner M belonging to the surrounding medium. On colliding with A^*, M instantaneously increases its kinetic energy to M' by carrying away the internal energy released by A^*. The microscopic origin of the temperature rise results form the amount of energy released to M. This two-step reaction can be schematically represented as:

Absorption: $A + h\nu \rightarrow A^*$ (vibronic)
Deactivation: $A^* + M(E) \rightarrow A + M'(E + \Delta E)$ (thermal)

For completeness, it should be mentioned that in standard thermodynamic conditions the kinetic energy per molecule, kT, is about 0.025 eV, whereas so-called thermal lasers such as CO_2, Nd:YAG, and argon, have corresponding photon energies 5 to 100 times larger (CO_2: λ = 10.6 μm; e = 0.12 Ev; Nd:YAG: λ = 1,060 nm; e = 1.17 Ev; Ar: λ = 514 nm; e = 2.4 Ev).

The photophysical parameter of interest is the absorption coefficient $\alpha(cm^{-1})$, which also measures the characteristic absorption length $1/\alpha$. This wavelength or frequency dependent coefficient $\alpha(\nu)$ is the product of the molecular absorption cross-section $\sigma(cm^2)$ and the number density n (number of homogeneously distributed absorbing molecules per unit volume,

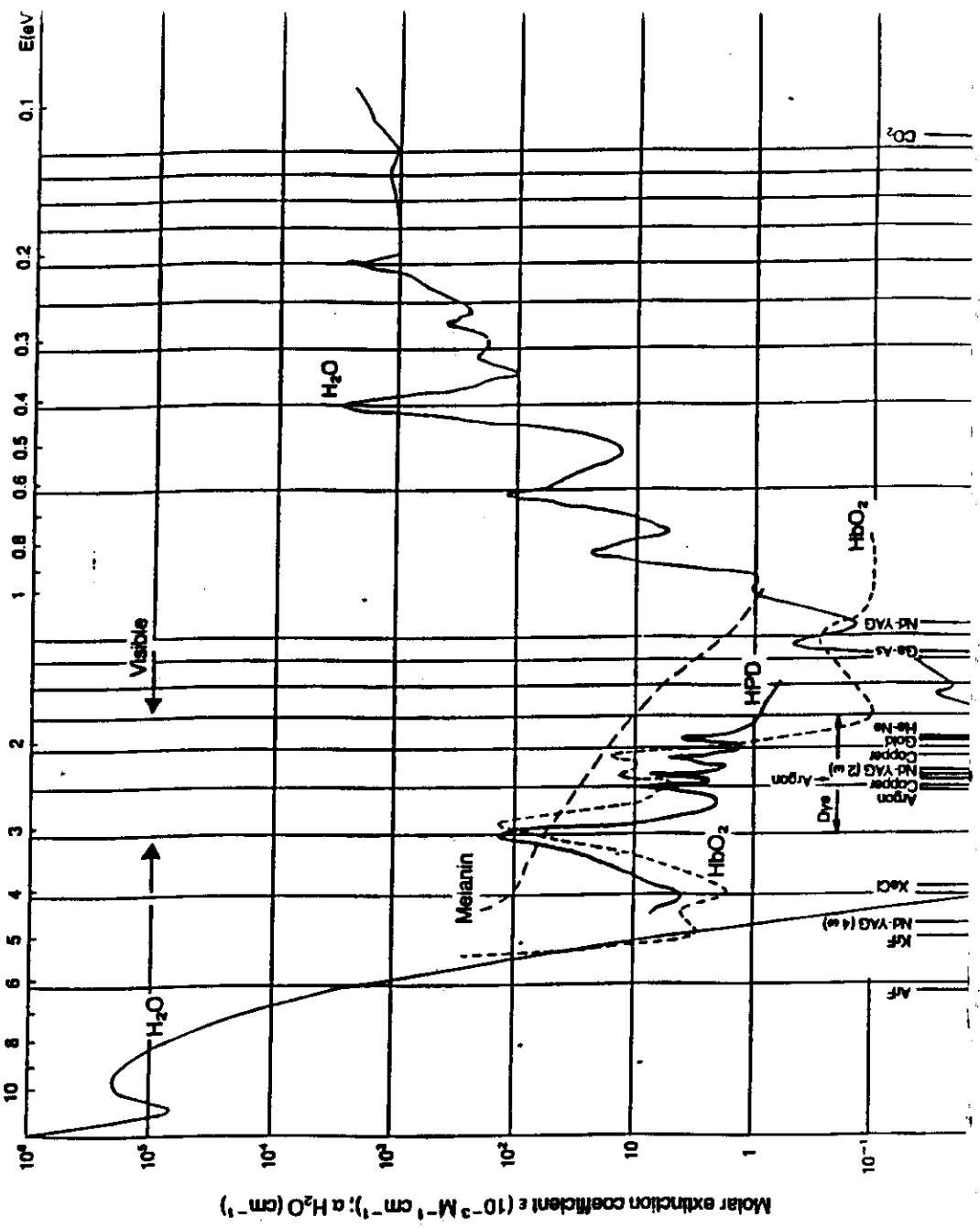

FIG. 11

measured in cm^{-3})

$$\alpha = \sigma n$$

The quantity σn is the absorbance. A more commonly used form of this law is:

$$I = I_0 10^{-\varepsilon c l}$$

where $\varepsilon(\nu)$, measured in 1/mol-cm, is the molar (decadic) extinction coefficient characteristic of each molecular species in a given solvent and c (mol/L) is the concentration of the absorbing substance.

The respective coefficients of water, oxyhemoglobin (HbO_2), adenine, and melanin are plotted in Fig.11 over a wide spectral range. Absorption of tissue in the UV varies drastically depending on the concentration of DNA and aromatic residues of proteins, but in general most organic molecules absorb very strongly in this range.

The water absorption coefficient, which typically reaches 10^6 cm^{-1} in the vacuum UV at 100 nm, exhibits a dramatic cutoff around 190 nm and has no significant absorption throughout the entire UV range. For physiologic saline, absorption starts below about 200 nm, reaching $\varepsilon \sim 300$ 1/mol-cm at 193 nm, the wavelength of the ArF excimer laser. This absorption is, however, due to Cl^- ions.

Nuclei acids, which constitute about 10% to 15% of a cell's dry weight, are the most widespread absorbers in the 190-300 nm spectral region.

Infrared radiation, on the other hand, is absorbed mainly by water with increasingly stronger bands toward longer wavelengths (300 cm^{-1} at 3 μm), with typical absorption depths as small as 10 μm in the far IR. Clearly, in Fig.11 a spectral therapeutic window is delineated between 600 nm and 1,200 nm. In this range, radiation penetrates tissues with fewer losses because of weaker scattering and absorption, thereby offering the possibility of reaching deep targets.

The first mechanism by which tissue is thermally affected is molecular denaturation (of, e.g., proteins, collagen, lipids, hemoglobin). For completeness, Table 3 summarizes the temperature ranges of successive transformations.

In the neighborhood of T ~ 45°C (hyperthermic range) one observes a tissue retraction related to macromolecular conformational changes, bond destructions, and membrane alterations. The range of protein denaturation is between 50°C and 60°C. As the molecule reaches its "melting temperature", the originally densely packed polynucleotide chain unfolds and a process called "chain melting" occurs, associated with a marked increase in light absorption around 260 nm.

Above the protein denaturation temperature, coagulation necrosis and vacuolation are produced. The temperature limit at which tissues become carbonized is about 80°C. Vaporization occurs beyond 100°C, predominantly from heated free water. The high vaporization heat of water (2,530 J/g) is advantageous, since the steam generated carries away excess heat, thereby preventing further temperature increase of adjacent tissue. Vaporization together with carbonization yield decomposition of tissue constituents.

The major problem with material removal is to adjust the duration of laser exposure in order to minimize tissue injury and thermal damage to adjacent zones so as to obtain little necrosis. The scaling parameter for this time-dependent problem is the so-called thermal relaxation time, τ, associated with a characteristic diffusion length L. From heat diffusion

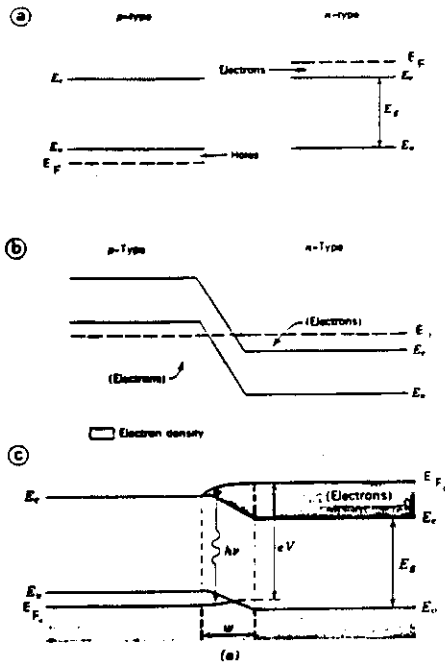

Fig. Band structure of heavily doped semiconductor and construction of a p-n junction. (a) Heavily doped semiconductors showing location of Fermi level E_F. (b) equilibrium band structure of p-n junction for degenerate material. (c) forward-biased p-n junction with recombination occurring in junction region.

Table 3 Histological Changes in Photothermal Processes

Conversion of Electromagnetic Radiation into Heat ↓ Elevation of Tissue Temperature	
43°C—45°C	Conformational changes Retractation Hyperthermia (cell mortality)
50°C	Reduction of enzyme activity
60°C	Protein denaturation Coagulation
80°C	Collagen denaturation Membrane permeabilization Carbonization
100°C	Vaporization and ablation

theory, this latter quantity can be shown to be proportional to the square root of time together with a lumped physical parameter, the tissue diffusivity K(cm^2/sec), characterizing the material thermal response (thermal conductivity, specific heat, and density). The relaxation time is then related to L through a relationship of the form:

$$L^2 = 4KT$$

For example, since the diffusivity of liquid water is $K = 1.43 \times 10^{-3}$ cm^2/sec, heat diffuses approximately to 0.8 mm in 1 sec in aqueous media. Similarly, typical thermal relaxation times associated with 10-μm vessels are on the order of 2×10^{-4} sec, whereas for microvasculature of 100-μm size they reach approximately 1.8×10^{-2} sec.

The relationship serves as the theoretical basis of a scheme, called selective photothermolysis, making use of pulsed irradiation to confine thermally mediated radiation damage to choose pigmented targets at the ultrastructural, cellular, or tissue structural level.

3.3 Photochemical

It is possible to schematically distinguish two subfamilies:

1. Reactions in which molecules are involved as energy carriers or as catalytic regulators after experiencing a photoexcitation. In this case the chromophore receptors are said to be photoactivated. One of the most attractive applications of this type is laser spectral sensitization in which photodynamic therapy (PDT) of malignant tumors appears to be a highly promising technique.

2. Reactions in which the chromophore molecules are modified and converted into photoproducts. An example of general importance is the photoinactivation caused by short-wavelength ultraviolet light used in the recently introduced technique of photoablative microsurgery.

A chromophore compound capable of causing light-induced reactions in molecules that do not absorb light in the same wavelength range may be called a photosensitizer. Following resonant excitation by a monochromatic source, the photosensitizer undergoes a series of simultaneous or sequential decays which result in intramolecular transfer reactions. The decays may ultimately culminate in the release of highly reactive cytotoxic species that cause, for example, irreversible oxidation of some essential cellular component and destroy affected host tissues. The essence of this photochemical interaction, which should rather be called photosensitized oxidation, lies in the "assistance" rendered by the exogenous chromophore receptor, which basically act as a photocatalyst. It is first activated by resonant absorption, thereby storing energy in one of its excited states; only when it deactivates, can a chain reaction take place, but with a reactant that is not the photosensitizer.

Typical photosensitization are hematoporphyrin derivative (HpD). Fig.12 presents the absorption spectrum of such compounds. The wavelength choice is also due to the need to penetrate deeply in the tissue. So that red radiation 600-700 is best considered to this purpose.

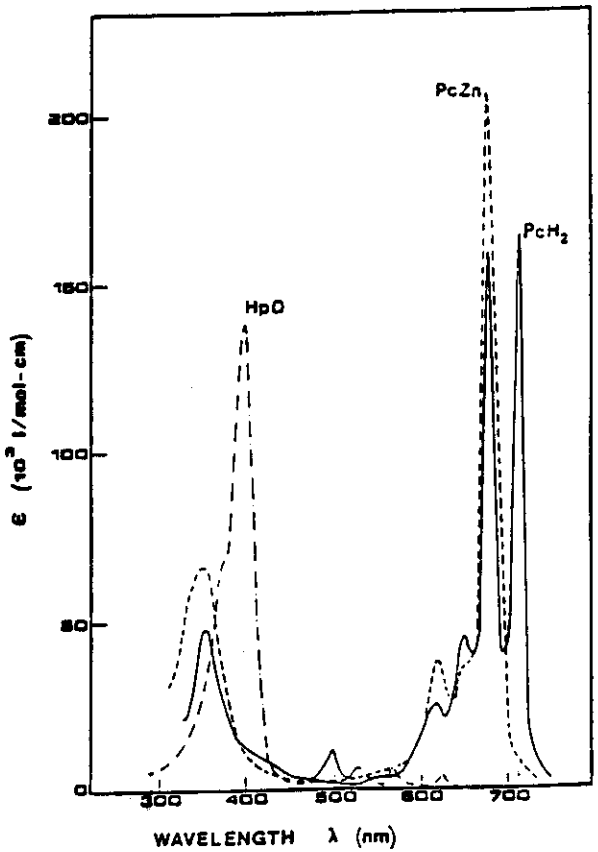

Figure 12. *Relative absorption spectra of hematoporphyrin derivative (HpD) and phthalocyanine in the spectral range 300 nm to 800 nm.*

3.4 Photomechanical

With this term is usually defined the mechanical interaction of the target with the acoustic wave associated to the transient absorption of a pulsed radiation. This type of effect becomes significant even at 1-10 J/cm^2 causing a characteristic vacuolization and ruptures of the tissue structures. Table 4 reports the physical principles laying behind this effect. Basically the laser pulse determines a plasma formation via a laser-induced breakdown. This sudden plasma formation couples a substantial energy to a spherical shock wave propagating in the surrounding media. If the irradiation site is submerged into water, the shock wave cannot expand freely and a strong recoil force is transmitted through the tissue bulk. If this force overcomes the strength linking together different portions of a composite structure such as an urinary calculus, it becomes possible to obtain a fragmentation in smaller pieces. This is what is called laser lithotripsy and it is entirely relying on the excitation of a photomechanical interaction process.

3.5 Photoablative

As already stated, UV radiation is very strongly absorbed by most biomolecules (Fig.11), specifically in a band extending from 200 nm to 320 nm.

Table 5 presents the sequence of effects induced by UV radiation and leading to photodissociation and the release of molecular scale fragments called ablation. This effect was first discovered and investigated by Srinivasan studying polymers laser irradiation in semiconductor processing. To the extent of being organic materials, both polymers such as PMMA, PVC, and other biological tissue behave in a very similar way when irradiated with UV radiation.

Because of the high quantum energy of this radiation (6.2 to 4 eV), it can modify and convert chromophores into photoproducts by photodissociation of functionally important compounds (proteins, nucleic acids, enzymes, pigments).

This feature has recently been exploited experimentally to produce well-defined, nonnecrotic, photoablative cuts of very small width (~ 50 μm) by exposure to excimer lasers at several UV wavelengths (ArF: 193 nm/6.4 eV; KrF: 248 nm/5 Ev; XeCl: 308 nm/4.3 Ev), with short pulses (15 nsec) focused on various tissues (cornea, skin, plaques). Typical irradiances are 10^6-10^9 watts/cm^{2}s. Similar sharp cuts (2-3 μm) with minimal thermal damage are also obtained with the 4th harmonic of the Nd:YAG laser at 266 nm (4.7 eV), with excellent cutting aspect owing to the high spatial quality of the beam. Control of thermal damage is clinically important since it generally produces undesirable biologic effects.

Fig.13 presents the typical curves determining threshold and saturation energy density levels for each substance. Table 6 reports the different threshold observed to ablate a typical tissue with the available excimer laser lines. It is interesting to notice that UV photoablation is inherently a pulsed process of 100 ns at most If a requirement of minimal thermal conduction from the irradiated zone to the bulk has to be fulfilled.

Generally speaking photoablation is a process which removes biological material with some very particular issues:

1) great depth control because each pulse etches only a few tens of microns.
2) A very limited part of the incoming energy is channeled into heat so that a limited rise

Table 4 Physical Principles of Laser-Induced Breakdown

• Short laser pulse focused at target	$I \sim \frac{(E_{ea}/\tau_{ea})}{W_s^2}$
↓	
• High power density	$I \sim 10^{12}$ W/cm^2
↓	
• High electric field	$E = \left(\frac{2}{c\varepsilon_0} I\right)^{1/2} \sim 10^8$ V/cm
↓	
• Dielectric breakdown (multiphoton process)	$E_{laser} \sim E_{\text{[illegible]}}$
↓	
• Plasma formation free electrons	$N_e \sim 10^{21}$/cm^3 $T > 20000$°C
↓	
• Spherical shock wave propagating at sound velocity	P (bars) $\sim 13\, E_{mJ} \frac{E_a(mJ)}{R(mm)}$ $A \sim 15\ 10^6$ mm/s
↓	
• Localized mechanical rupture for small radius	P > Yield strength of tissues

Table 5 Physical Principles of Laser Photoablation

• Short U.V. laser pulse (10 nsec) focused on tissue	$I \sim 10^8$ W/cm^2
↓	
• Strong absorption in the U.V. (6eV) (proteins; amides; peptides)	Absorption depth ~ 1 μm
↓	
• Promotion to repulsive excited state	
↓	
• Photodissociation	
↓	
• Desorption	
↓	
No necrosis	

TABLE 6 *Normal Aorta Penetration Depths and Limiting Repetition Rates for a Beam Radius of 0.2 mm, Using the Penetration Depths of Furzikov [5]*

Laser	Wavelength (nm)	Penetration depth (μm)	Limiting repetition rate (Hz)	Ablation threshold J/cm^2
ArF	193	1	37,000	0.05
KrF	248	15	156	0.4
XeCl	308	50	15	1.3
Dye	465	384	8.3[a]	10
Ar	514.5	313	8.3[a]	--
Nd:YAG	1,064	1,400	8.3[a]	37
Er:YAG	2,940	2	9,260	0.05
CO_2	10,600	20	93	0.5

[a] Pulse width (t_p) is assumed to be (much) less than three times the relaxation time, Equation (16). Again, the possible occurrence of tissue bond breaking and/or shock-wave generation is neglected.
[b] Limiting repetition rate governed by beam radius.

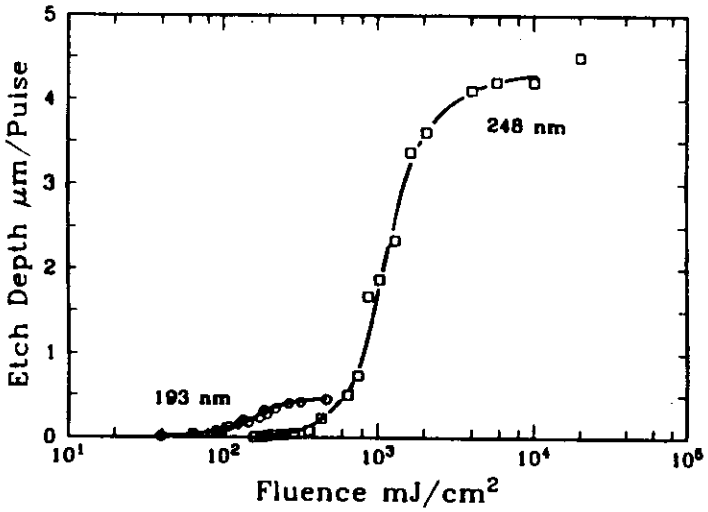

FIG. 13

FIG. 14
A : VIS LASER
B : UV LASER

of temperature takes place at the border

3) Very clean and sharp edges cuts or holes can be obtained in almost all types of tissues. Fig.14 presents a comparison of holes obtained with UV and VIS lasers to appreciate the difference.

4. Radiation delivery systems & surgical laser requirements

For every laser source proposed for a biomedical application it is of outstanding importance to rely on a suitable beam delivery system capable of the most convenient utilization of the laser energy at the site of the irradiation, preserving all the necessary characteristics of the beam. In other words main requirements for a delivery system are: 1) good transmission efficiency; 2) good beam focussability; 3) easy to manipulate. In this respect both free or guided propagation can provide adequate solutions.

4.1 Optical fibers

In practice optical fibers constitute an almost ideal solution in terms of transmission efficiency, compactness, flexibility, low cost and so on. The only limitation is due to the typical transmission window for each material constituting the core of the fiber. Fig.15 presents the typical transmission curve of silica fibers. As it can be seen a reasonable transmission is obtained only in the range 0.25-2 μm.

For lasers with an emission wavelength external to this other solutions can be considered. A large effort is presently devoted to IR fibers for transmission in the range 2-10 μm. ZrF_4, and other fluoride glasses are proposed near 3 μm, Thallium and Silver halides have been proposed for 10 μm, even if the former are highly toxic and the latter are still experimental. Crystalline fibers are under study to solve the IR transmission problems. An important issue for laser power and energy delivery is the maximum level coupled into the fiber without causing a permanent and catastrophic damage. CW lasers in this respect do not suffer this damage limitations because very high CW power can be easily transmitted through suitable fibers. This is the case for Nd:YAG lasers which can easily transmit 100 W and more through a 600 μm fiber. Similar situation for Ar ion lasers especially considering that for medical applications much lower power are needed. Problems have been instead observed for pulsed lasers. In fact the very high peak power exerted by Q-switch operation can rise the instantaneous power density at the entrance face of the fiber up to 4 W/cm^2 reaching the threshold for a surface breakdown which cause a severe acoustic and thermal damage which usually breaks the fiber. Sometimes, high quality beams impinging a fiber with a power density lower than the damage can cause problems inside the bulk of the fiber because of internal reflections. Another class of effects which can cause permanent damage to the fibers is due to the powerful shock wave excited on the target in a liquid environment (opaque or transmitting).

4.2 Articulated arms

For laser emitting out of the range 0.25-2 μm it is possible to use an articulated arm to

SPECTRAL ATTENUATION FIG. 15

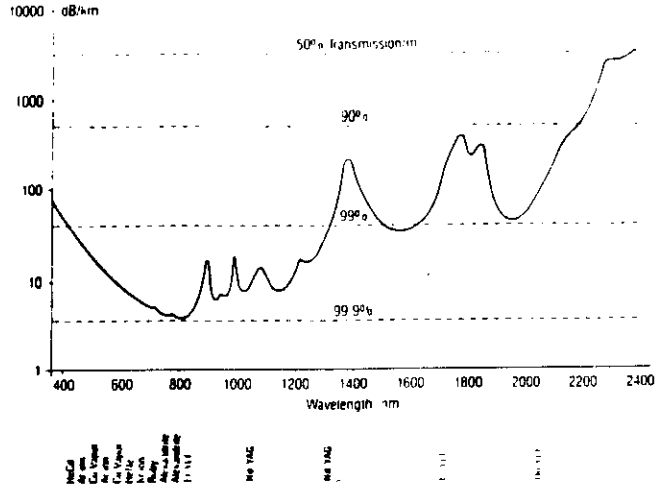

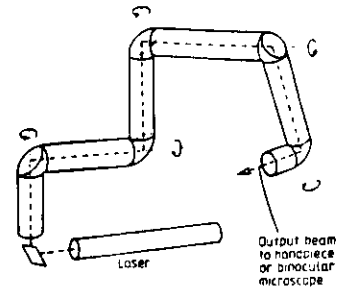

Figure 16 The CO_2 laser beam can be aimed in all directions by mirrors in the rotating joints of an articulated arm.

provide both high transmission efficiency and a reasonable ease to manipulate the beam. Fig.16 presents a solution with 6 arms and 5 rotating joints. A mirror set at 45° in each joint keeps the beam centered in all the arms transmitting the beam to a final hand piece operated by the surgeon. Here a lens focus the beam a few mm out of the hand piece. This type of articulated arm is typical of surgical CO_2 laser and an example is reported in Fig.1.

A similar need is also present for ArF excimer laser. This laser emits at 193 nm high power pulses which are useful in ophthalmology and in this case an articulated arm is provided to connect the laser device to the irradiation site.

5. Biomedical applications : Basic concepts

In this review I will focus on the basic concepts suggesting the biomedical application of a particular type of lasers, rather than on the pathologies and the clinical aspects which can be better described in specific literature.

5.1 Ophthalmology

The possibility to use laser light as useful tool in eye surgery was soon proposed to substitute Xenon lamps for retinal pathologies. Later several other laser procedures have been introduced also for diseases of the anterior chamber of the eye. Briefly the present use of lasers can be divided in three categories:

1) retinal photocoagulations
2) cataract surgery
3) corneal reshaping

In the first the aim to photocoagulate hemorrhagic site or to point welding of detached retina is based on the choice of lasers wavelengths which can be highly absorbed by the blood vessels or by pigmented tissue. To this extent Argon ion lasers emitting in the blue-green can be favorably employed considering also that CW radiation can better provide small size burns needed for such applications, without providing mechanical damage as a pulsed emission can do. So since their introduction in 1968 surgical Argon laser suitably coupled to a slit lamp have been satisfactorily used for retinal photocoagulations and generally speaking for all the retina surgery. For macular lesions Krypton ion laser in the red have been instead employed to limit the risk of unintentional photocoagulations. Recently laser diode at 900 nm have been also proposed to produce similar burns with an extremely simplified laser source.

The cataract surgery needs differently a pulsed laser emission, well transmitted by the cornea, to shut the opacified lens capsule to restore the vision opening a window by mechanical disruption. Q-switched Nd:YAG lasers suitably focussed on the target have been used to this purpose with energies between 8 and 16 mJ in pulses of 12 ns.

Corneal reshaping is a very recent experimental technique to correct myopia by several methods. They are based essentially on very fine and precise incisions made possible by excimer laser ablation of the cornea. Radial keratectomy provide several (6-8) cuts on the cornea out of the iris to release the internal forces and to decrease the curvature and the optical power. Later a more proper corneal reshaping has been proposed in which the correction is achieved by a centered ablation in the shape of a step negative diopter. Fig.17

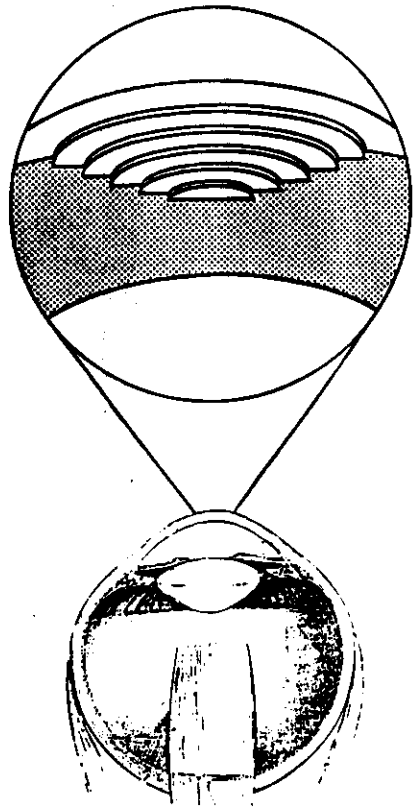

FIG. 17

presents a scheme of this procedure. The correction is readily achieved removing just a few tens of microns.

5.2 Endoscopic surgery

In the chest medicine the role of lasers is essentially in the diagnosis and treatment of malignant and non-malignant diseases. CO_2 lasers can be employed for short propagation paths such as the ones related to the tracheobronchial tree. In this case treatments are performed through a bronchoscope allowing a direct vision of the irradiation site. The high absorption of the 10.6 μm radiation can easily remove even large tumoral masses, but typically the hemostatic effect useful to reduce the blood loss is not relevant. Better results can be generally be obtained using Nd:YAG for several reasons: 1) the use of optical fiber to transmit the radiation allows the construction of flexible catheters to reach in endoscopy the target site in a much more extended number of fields: gastrointestinal vascular lesions, palliation of esophageal carcinoma, biliary tract, gastric tumors, colon and rectum, gynecology and urology.

5.3 External surgery

Several different surgery specialities could be included, here I prefer to consider all in dermatology. The role of lasers in dermatology can be divided as follows:
1) the Argon laser in the treatment of the port wine stain and other vascular abnormalities of the skin,
2) the CO_2 laser in the treatment of skin lesions
3) the ruby laser in the treatment of pigmented skin lesions
4) laser biostimulation of healing wounds

Once again Argon laser propose its blue-green radiation for highly absorbing vascularized tissue. This is the case of port wine stain which can be popped out spot by spot with proper irradiations, photocoagulating the vessels net and producing a marked lightening of the stain. CO_2 lasers are preferably used for external surgery whenever a high precision, bloodless light scalpel is needed. One example are severely and extensively burned regions. Ruby laser has been used to remove tattoos or to treat and remove pigmented spots.

Since 1960 Mester and coworkers reported biostimulation of hair growth, collagen synthesis and capillary growth under irradiation with low power He-Ne laser radiation. There is at present, insufficient evidence to confirm these findings and more careful controlled clinical trials are essential.

5.4 Photodynamic therapy

Before discussing in detail the development of this technique it is essential to outline, simply, its mode of action. The photosensitizer hematoporphyrin derivative (HPD) is administered to the patient by intravenous injection in a dose of 3 mg kg^{-1}. After injection this substance is widely distributed within the body tissues but is then selectively retained by malignant tumors. Therefore, by the third day after injection, the HPD has been cleared from normal tissues, but still retained by malignant tissues. At this stage it can be used either to

diagnose or to treat tumors. When exposed to blue light, the tumor containing HPD will fluoresce red enabling malignant tissues to be identified. If the tumor is exposed to red light at a wavelength of 630 nm, singlet oxygen is produced by energy transfer from the excited porphyrin molecule and this is cytotoxic causing destruction of the malignant tumor without damage to the surrounding normal tissues, which do not contain HPD.

Although photoradiation therapy, which is now often referred to as photodynamic therapy, cannot, in its present form, represent a panacea for cancer, it must be an important therapeutic modality for many forms of malignant disease.

Table 7 presents the physical principles.

The primary target (or targets) is as yet not certain, but it would appear that tumor destruction is caused by both vascular and cellular effects. Weishaupt et al. (1976) have shown that when HPD is photoactivated, singlet oxygen is produced. This is a highly reactive transient state of the oxygen molecule which is cytotoxic as a result of oxidizing sensitive cellular targets.

Recent measurements have in fact shown that elevation of the tissue temperature induced by PDT laser treatment could also contribute to cell destruction. This role of hyperthermia in enhancing tumor control has been tested by monitoring sequential PDT treatments and localized microwave irradiation in vivo. The results suggest that the tumor response to photodynamic therapy was enhanced both by sublethal hyperthermic treatment (30 min at 40.5°C or 41.5°C) and by a moderately lethal heat treatment (30 min at 44.5°C).

A wavelength of 630 nm has been defined as the optimum wavelength for PRT at present, as it activates HPD and penetrates adequately into tissues. It would obviously be preferable to utilize a wavelength such as that of the Nd:YAG laser which penetrates further but no sensitizers at that wavelength have yet been found.

A number of studies of light penetration have been carried out and the depth of tissue penetration to create a fall in light intensity of 37% has been calculated, but it has been shown that photoactivation can occur to a greater depth than this. The penetration will depend, to some extent, on the consistency and homogeneity of the tumor, but for many tissues an effective penetration of up to 1 cm can be achieved..

Clinical application has been extended so far to cases regarding several tumors sites: bladder, breast cutaneous metastases, brain. gastrointestinal tumors, gynecology, head and neck, lung, ocular tumors, skin.

5.5 Laser angioplasty

Between the endoscopic treatments the proposal of using high power laser light to recanalize occluded arteries came out relatively late(10). Here the basic idea has been to take full advantage of at least three laser radiation capabilities:
1)to drill neo-lumina through atherosclerotic plaques,
2)potential delivery by means of optical fibers,
3)excitation of plaque autofluorescence, collected back through the fiber for a real time recognition and a guiding aid during the treatment.

The scheme of an intra-operatory coronary angioplasty is shown in fig.18. Also a percutaneous pathway has been proposed to reach safely an occluded site in the coronary district, to recanalize the plaque providing an adequate neo-lumen for a sufficient hematic flux.

Table 7 Photosensitization Kinetics in Type I and Type II Mechanisms and Possible Carotenoid Protection

Resonant excitation	
1. Singlet state absorption	$^1S + h\nu \rightarrow {}^1S^*$
Decays	
2. Radioactive decay (fluorescence)	$^1S^* \rightarrow {}^1S + h\nu'$
3. Nonradioactive singlet decay	$^1S^* \rightarrow {}^1S$
4. Intersystem crossing	$^1S^* \rightarrow {}^3S^*$
5. Triplet state decay	$^3S^* \rightarrow {}^1S$
6. Triplet phosphorescence decay	$^3S^* \rightarrow {}^1S + h\nu^*$
TYPE I MECHANISMS	
Free radical derivations	
7. Hydrogen transfer	$^3S^* + RH \rightarrow SH^* + R^*$
8. Electron transfer	$^3S^* + RH \rightarrow S^{-\cdot} + RH^{+\cdot}$
	$^3S^* + RH \rightarrow S^{-\cdot} + RH^{+\cdot}$
Reactant formations	
9. Peroxiradicals	$R^* + O_2 \rightarrow RO_2^*$
	$RH^{+\cdot} + O_2 \rightarrow H^+ + RO_2^*$
10. Superoxide anion	$RH^{+\cdot} + O_2 \rightarrow RH + O_2^*$
	$e_{aq}^- + O_2 \rightarrow O_2^{-\cdot}$
Oxidation	
11. Substrate stabilization	$RH, RO_2^* \rightarrow R(O_2)$
TYPE II MECHANISM	
Reactant formation	
7. Intermolecular exchange	$^3S^* + {}^3O_2 \rightarrow {}^1S + {}^1O_2$
Oxidation	
8. Cellular oxidation	$^1O_2 + X \rightarrow X(O)$
CAROTENOID PROTECTION	
1. Singlet oxygen extinction	$^1O_2 + {}^1CAR \rightarrow {}^3O_2 + {}^3CAR$

Sensitizer s: ^1S singlet ground-state: $^1S^*$, excited singlet state: $^3S^*$, excited state. Oxygen O_2: $^3O_2$, triplet ground-state: $^1O_2$, excited singlet state. Substrate RH: $R(O_2)$, stable oxidized form. Cellular target X: X(O), oxidized target. Carotenoid CAR: ^1CAR, singlet ground-state: ^3CAR, excited triplet state.

Table 7 Physical Principles of Photodynamic Therapy

- Administration of photosensitizer S
- Selective tumor retention of photosensitizer
- Irradiation by monochromatic source (laser)
- Resonant excitation of Photosensitizer

$$S + h\nu \longrightarrow S^*$$

Simultaneous or sequential decays

Intramolecular transfers	Thermal deactivation
Production of reactive species	
Cytotoxic action	Hyperthermia

Tumor Eradication

FIG. 18a

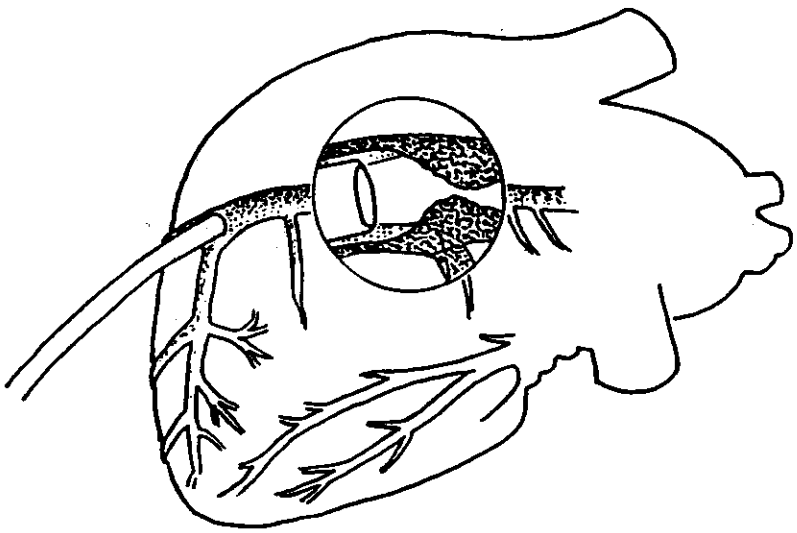

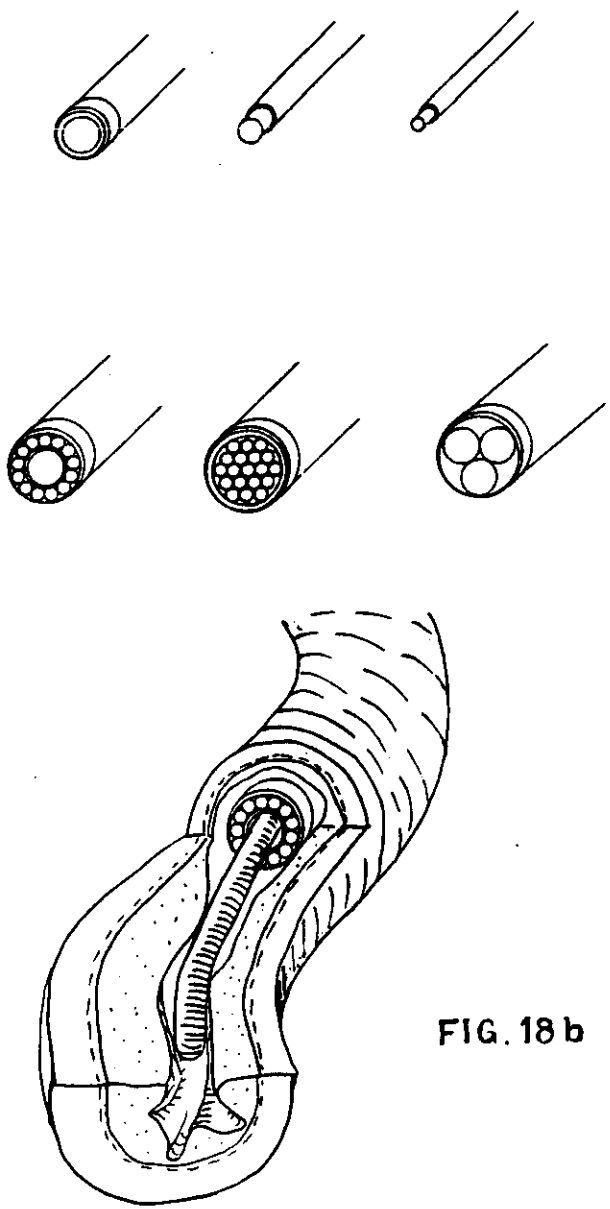

FIG. 18 b

As it can be easily understood the relevance of this therapy for coronaropathy would be very high if demonstrated, because it is less invasive and more convenient than aorto-coronary by-pass procedures.

Summarizing this goal requires some crucial achievements:

1) a laser light interaction model (with the composite plaque structure) capable of material removal without bubbling, embolism or other potentially counter-productive effects,

2) an optical catheter design ensuring maximum flexibility to follow the natural sinuosity of coronary arteries.

In this respect, since the pioneering experiments of laser angioplasty, the laser choice was mainly driven by the availability of laser types which were well known to the biomedical community because of other applications. The propagation through fibers excluded CO_2 lasers limiting to Ar+ and Nd:YAG lasers the possible choice. With them the material removal process was essentially a thermal one and a more or less pronounced damage was reported by many authors in vitro and in animal model, limiting the clinical application to large peripheral vessels and excluding any practical coronary approach.

Since 1984 the unique properties of ultraviolet ablation have given new perspectives to this field, providing positive answers to the main requirements:

1)photochemical ablation with negligible thermal damage

2)good optical fiber transmission @308 nm,

3)guiding aid possible by autofluorescence excitation.

Table 6 represents thresholds for different lasers. A high absorption coefficient implies a small penetration depth and a consequently small volume involved. The energy requirement is proportional to the mass and these simple relationships justify the low threshold values observed in the UV or under the water absorption peaks @ 2.9 μm. For this reason analogous ablation properties are attributed to radiation emitted at that wavelength from HF or Er:YAG laser. Yet the lack of suitable fibers at 3 μm (ZrF_4 and other fluorides glasses are brittle, expensive and require a more advanced production technology) and the unavoidable screening effect provided by even small water layers in a wet environment such as in a percutaneous scenery, reduce the effectiveness of this proposal.

Anyhow problems are being faced in the excimer lasers biomedical experimentation too. Some of them are related to high power coupling in optical fibers. In facts standard short pulse excimer laser provide energy density of several J/cm^2 by a suitable focussing of the beam, with an inherent peak power density of the same order of magnitude needed to induce optical breakdown on the input face of the fiber. To increase the reliability of high power delivery through optical fibers in the ultraviolet long pulse excimer laser have been proposed. In such a way the energy is provided with a lower power density coupled into the fiber. Or conversely, a larger amount of energy can be coupled within a reasonable fraction of the damage level. This energy coupling capability has been found proportional to the square root of the pulse duration. From a comparison of the available wavelengths the XeCl excimer at 308 nm turns out to be the most favorable from several points of view:

1) best compromise between low ablation threshold and power fiber coupling,
2) longer current pulse stability than fluorides,
3) quite affordable fiber propagation loss,
4) less engineering problems than fluorides.

In vitro ablation experiments pointed out soon that flexibility requirement asked for a

composition of multiple fibers to achieve a relatively large diameter optical catheter. In facts the limited amount of energy coupled in a thin fiber is not sufficient to irradiate a much larger target area. On the other hand, in coronary and even more in peripheral recanalizations satisfying neo-lumina are in the order of 2 mm.

With excimer lasers optical catheter engineering is tightly related to the laser performance itself. For a pulse duration of 100 ns an energy density of 3 to 5 J/cm2 can be reliably coupled. This level is a factor two or three higher than the ablation threshold. Whatever is the catheter geometry such a factor is necessary to overcome the unavoidable not "optically active" space between closely packaged fibers. For the catheter progression in facts the overall output radiation lobe has to irradiate (with at least 1.5 J/cm2) an area comparable in size with its own dimension. Fig.19 shows the scanning electron microscope presentation of the hole drilled in aortic wall during in vitro experiments, by means of a 3x600 μm core fibers.

The need for a suitable overposition remains outlined. the pioneering work performed by Laudenslager and Grundfest has led to subsequent very effective "over the wire" optical catheters. Employing single fibers of 200 μm or even less, the overall flexibility has been demonstrated suitable for percutaneous coronary treatments. Our experience in the field has been so far extended to clinical trials performed in coronary arteries as an assist to A.C. by-pass procedures and in peripheral arteries through the percutaneous pathway. Neo lumina of 2 mm in diameter has been successfully obtained through lipid-rich plaques, while negligible results have been observed in heavily calcified ones. Other authors report successful recanalization with energy doses higher than 3 J/cm^2.

In our experiments the laser system was developed under the sponsorship of a Special Project of the Italian National Research Council. The clinical trials are being conducted in the Cardiovascular Surgery Institute of the Padua University and at the Laser Angioplasty Section of the USL 10/D in Florence. The device is shown in fig.20, it has a 80 ns FWHM pulsewidth and an emission energy of 120 mJ. Fibers coupling provide up to 4 J/cm2 at the fiber output. Fig.21 presents a typical occlusive plaque localized in the phemoral artery successfully recanalized by the excimer laser angioplasty treatment and no subsequent balloon dilatation.

Presently the groups active in the field are reaching thousands of treatments worldwide. Multiple center trials started in 1988 and soon a several years follow-up will be available to disclose less investigated long term problems such as the restenosis rate.

Following the general concept of autofluorescence utilization for the recognition of biological tissues, laser induced fluorescence LIF was also proposed as a diagnostic aid in angioplasty. Kittrell and Feld associated the spectroscopic technique to a multifiber catheter architecture devising a sort of real time "spectroscopic" endoscope. In their experiments suitably pulsed Ar+ lasers were mainly employed. The demonstrated discrimination between healthy artery wall and atherosclerotic plaque spectra triggered a wide interest in developing laser angioplasty systems provided with a similar capability. Some designs used He-Cd as the LIF pump laser. Later the successful utilization of excimer lasers promoted the use of the UV line itself for LIF excitation, to obtain a complete integration of the diagnostic technique with the laser ablation process for a real time recognition of the irradiated plaque consumption. Fig.22 shows typical fluorescence spectra emitted from a healthy wall sample compared with a lipid-rich or calcified plaque samples under operative laser fluence. Extensive in vitro experimentations have been reported, using different UV laser lines to excite the native fluorescence or chlorotetracycline-induced fluorescence. This compound binds preferentially

FIG 19

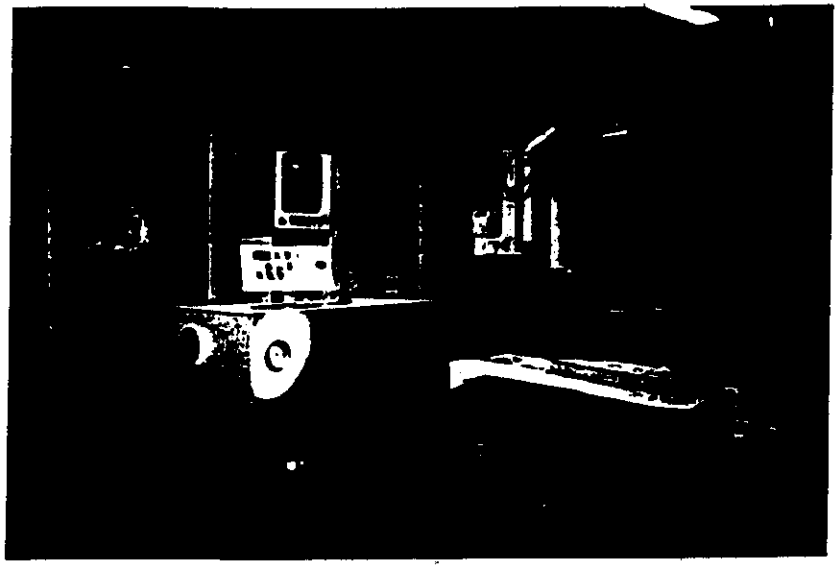

FIG. 20

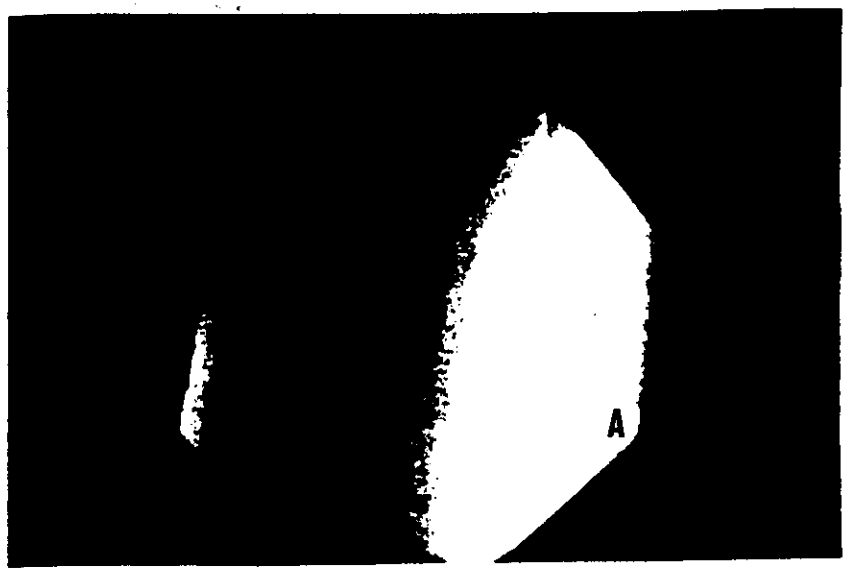

FIG. 21

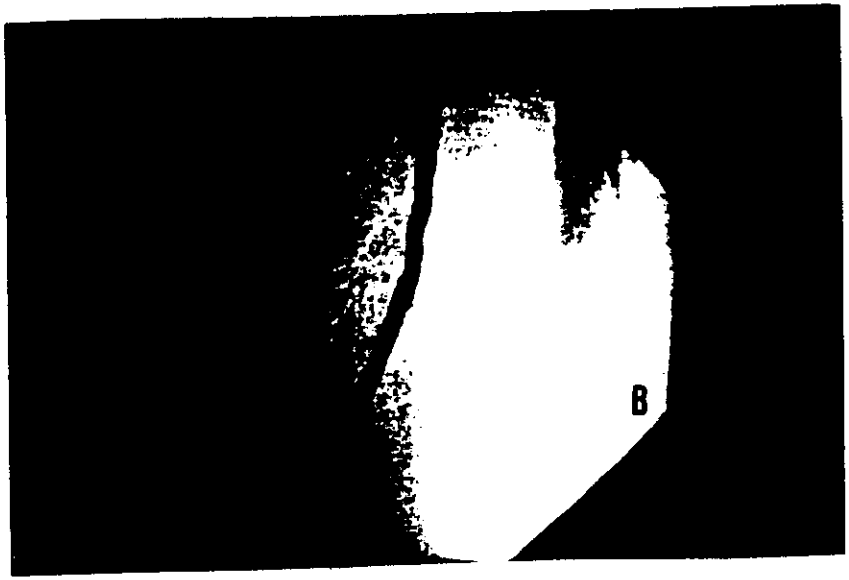

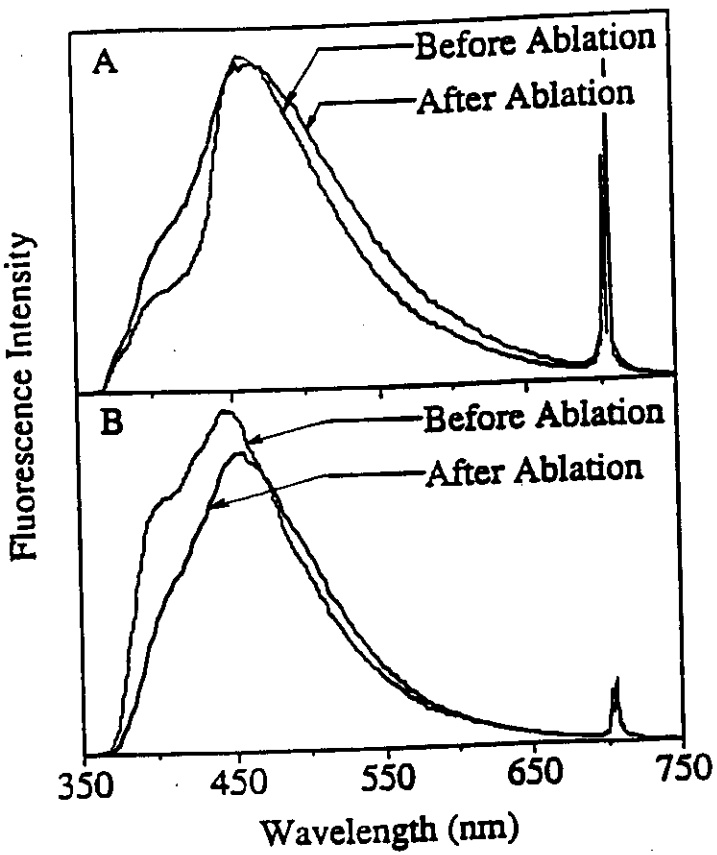

FIG. 22
A HEALTHY
B CALCIFIED

to divalent cations such as Ca++ in plaques, determining a discrimination factor enhancement.

Besides the scientific interest, clinical use of these methods on a routine basis requires a real time response of immediate utilization by the surgeon (or in automatic mode) to modulate the laser emission and to avoid "laser perforations" of the artery wall. As a matter of fact, present clinical results assign a minor failures contribution to laser perforations against mechanical ones, depending more on the catheter rigidity itself. Nevertheless a more mature laser angioplasty technology could find extremely convenient in the next future to associate LIF techniques as a guiding and targeting aids. Worth to be mentioned in this respect are other diagnostic competitors such as microendoscope for direct visualization and ultrasound imaging which could give even more complete information on the "in depth" plaque composition.